Published in final edited form as:

Cancer Res. 2017 April 15; 77(8): 2161–2172. doi:10.1158/0008-5472.CAN-16-2066.

Cyp24a1 Attenuation Limits Progression of *Braf*^{V600E}-Induced Papillary Thyroid Cancer Cells and Sensitizes Them to BRAF^{V600E} Inhibitor PLX4720

Minjing Zou[#1], **Essa Y. Baitei**[#1], **Huda A. BinEssa**[1], **Futwan A. Al-Mohanna**[2], **Ranjit S. Parhar**[2], **Rene′ St-Arnaud**[3], **Shioko Kimura**[4], **Catrin Pritchard**[5], **Ali S. Alzahrani**[6], **Abdullah M. Assiri**[7], **Brian F. Meyer**[1], and **Yufei Shi**[1]

[1]Department of Genetics, King Faisal Specialist Hospital and Research Centre, Riyadh, Saudi Arabia. [2]Department of Cell Biology, King Faisal Specialist Hospital and Research Centre, Riyadh, Saudi Arabia. [3]Department of Surgery and Human Genetics, McGill University, Montreal, Quebec, Canada; and Research Centre, Shriners Hospitals for Children, Montreal, Quebec, Canada. [4]Laboratory of Metabolism, National Cancer Institute, National Institutes of Health, Bethesda, Maryland. [5]Department of Biochemistry, University of Leicester, Lancaster Road, Leicester, UK. [6]Department of Medicine, King Faisal Specialist Hospital and Research Centre, Riyadh, Saudi Arabia. [7]Department of Comparative Medicine, King Faisal Specialist Hospital and Research Centre, Riyadh, Saudi Arabia.

[#] These authors contributed equally to this work.

Abstract

CYP24A1, the primary inactivating enzyme for vitamin D, is often overexpressed in human cancers, potentially neutralizing the antitumor effects of calcitriol, the active form of vitamin D. However, it is unclear whether CYP24A1 expression serves as a functional contributor versus only a biomarker for tumor progression. In this study, we investigated the role of CYP24A1 on malignant progression of a murine model of *Braf*^{V600E}-induced papillary thyroid cancer (PTC). Mice harboring wild-type *Cyp24a1* (BVE$^{Cyp24a1\text{-}wt}$) developed PTC at 5 weeks of age. Mice

Corresponding Author: Yufei Shi, King Faisal Specialist Hospital and Research Centre, MBC#3, P.O. Box 3354, Riyadh 11211, Saudi Arabia. Phone: 966-1-4424768; Fax: 966-1-442-4585; yufei@kfshrc.edu.sa.

Authors' Contributions

Conception and design: M. Zou, E.Y. Baitei, R.S. Parhar, Y. Shi

Development of methodology: M. Zou, E.Y. Baitei, R.S. Parhar, R. St-Arnaud, C. Pritchard, A.S. Alzahrani, Y. Shi

Acquisition of data (provided animals, acquired and managed patients, provided facilities, etc.): M. Zou, E.Y. Baitei, H.A. BinEssa, R.S. Parhar, A.M. Assiri, Y. Shi

Analysis and interpretation of data (e.g., statistical analysis, biostatistics, computational analysis): M. Zou, E.Y. Baitei, H.A. BinEssa, F.A. Al-Mohanna, R.S. Parhar, B.F. Meyer, Y. Shi

Writing, review, and/or revision of the manuscript: M. Zou, F.A. Al-Mohanna, R.S. Parhar, S. Kimura, A.S. Alzahrani, A.M. Assiri, B.F. Meyer, Y. Shi

Administrative, technical, or material support (i.e., reporting or organizing data, constructing databases): E.Y. Baitei, H.A. BinEssa, R.S. Parhar, S. Kimura, C. Pritchard, A.M. Assiri, Y. Shi

Study supervision: R.S. Parhar, Y. Shi

Other (overall discussion and ongoing supervision): R.S. Parhar, Y. Shi

Supplementary data for this article are available at Cancer Research Online (http://cancerres.aacrjournals.org/).

Disclosure of Potential Conflicts of Interest

No potential conflicts of interest were disclosed.

harboring a homozygous deletion of *Cyp24a1* ($BVE^{Cyp24a1\text{-}null}$) exhibited a 4-fold reduction in tumor growth. Notably, we found the tumorigenic potential of $BVE^{Cyp24a1\text{-}null}$-derived tumor cells to be nearly abolished in immunocompromised nude mice. This phenotype was associated with downregulation of the MAPK, PI3K/Akt, and TGF|3 signaling pathways and a loss of epithelial-mesenchymal transition (EMT) in $BVE^{Cyp24a1\text{-}null}$ cells, associated with downregulation of genes involved in EMT, tumor invasion, and metastasis. While calcitriol treatment did not decrease cell proliferation in $BVE^{Cyp24a1\text{-}null}$ cells, it strengthened antitumor responses to the $BRAF^{V600E}$ inhibitor PLX4720 in both $BVE^{Cyp24a1\text{-}null}$ and $BVE^{Cyp24a1\text{-}wt}$ cells. Our findings offer direct evidence that *Cyp24a1* functions as an oncogene in PTC, where its overexpression activates multiple signaling cascades to promote malignant progression and resistance to PLX4720 treatment. *Cancer Res; 77(8); 2161–72*.

Introduction

Papillary thyroid cancer (PTC) is the most common type of thyroid cancer, accounting for more than 80% of thyroid cancer cases (1). The $BRAF^{V600E}$ mutation is the most frequent genetic alteration in PTC, occurring in 28% to 83% of cases with an average rate of 44% (2–4). Constitutive activation of the RAS-RAF-MEK-ERKMAP kinase signaling pathway (MAPK) promotes the initiation and progression of PTC.

Vitamin D is mainly involved in bone and mineral metabolism. It has other important functions, such as the modulation of cell growth and immune function (5). Its antiproliferative effects have attracted great enthusiasm in recent years for its potential application as an anticancer agent. Significant antiproliferative effects have been observed in many human cancer cells, including thyroid, prostate, breast, colorectal, and lung cancers (6–9). Vitamin D receptor (VDR) knockout mice displayed a higher incidence of carcinogen-induced breast and skin tumors (10), and vitamin D deficiency promotes human breast cancer growth (11). Although clinical trials have shown the potential therapeutic effects of calcitriol in prostate cancer patients (12), the success has not been convincing regarding the clinical effects of vitamin D or its analogues in cancer treatment (13,14). This may be due to the overexpression of *CYP24A1* in many cancer patients.

Vitamin D 24-hydroxylase *(CYP24A1*) is the primary vitamin D-inactivating enzyme, which catabolizes 1a, $25(OH)_2D_3$ (calcitriol) and, to a lesser extent, $25(OH)_2D_3$by24hydroxylationinto inactive 1a, $24,25(OH)_3D_3$ and $24,25(OH)_2D_3$ (6). The calcitriol-mediated antiproliferative effects could be disrupted by *CYP24A1* overexpression during tumor development (7). Indeed, *CYP24A1* overexpression has been observed in many cancers, including thyroid (15, 16), lung (17), colon (18), esophageal (19), and breast (20), and has been linked to poor prognosis in patients with lung (21), esophageal (19), colon (22), and thyroid (16, 23) cancers. It has been proposed as a candidate oncogene due to its gene amplification in breast cancer (24). In patients with thyroid cancer, the serum calcitriol level was found to be significantly lower (25), although there was no significant difference in the serum $25(OH)\ D_3$ level between thyroid nodule and thyroid cancer patients (25,26), indicating that calcitriol might be converted to inactive 1a, $24,25(OH)_3D_3$ by increased *CYP24A1* expression. Although these data suggest that *CYP24A1* overexpression

could result in the abrogation of calcitriol-mediated growth arrest leading to tumor development and/or progression, there are no *in vivo* functional studies to support this hypothesis.

In our previous study, we demonstrated that *CYP24A1* overexpression was associated with $BRAF^{V600E}$ mutation and advanced stages of PTC (23). We also showed that $BRAF^{V600E}$ induced *CYP24A1* overexpression and the $BRAF^{V600E}$ inhibitor PLX4720 significantly enhanced the antiproliferative effects of calcitriol in thyroid cancer cell lines (23). However, it is not clear to what extent *CYP24A1* overexpression contributes to thyroid cancer development and progression *in vivo*, especially in the presence of $BRAF^{V600E}$. In the present study, we used a mouse model of $Braf^{V600E}$-*induced* PTC to investigate the role of *Cyp24a1* in thyroid cancer progression. We observed that thyroid cancer growth was significantly reduced in the absence of *Cyp24a1* expression.

Materials and Methods

Animals

The generation of *TPO-*$Braf^{V600E}$ and *Cyp24a1* knockout mice ($Cyp24a1^{nuU}$) have been described previously (27–29). TPO-$Braf^{V600E}$ mice with wild-type *Cyp24a1* ($BVE^{Cyp24a1\text{-}wt}$) developed PTC at approximately 5 weeks of age and were used as PTC tumor controls. *TPO-*$Braf^{WT}$ mice with wild-type *Cyp24a1* were used as normal controls. *TPO-*$Braf^{V600E}$ mice with *Cyp24a1* knockout ($BVE^{Cyp24a1\text{-}null}$) were obtained by several rounds of breeding among *LSL-*$Braf^{V600E}$(30) *TPO-Cre* (31), and $Cyp24a1^{+/-}$ mice. Because 50% of the homozygous mutant $Cyp24a1^{null}$ mice died before 3 weeks of age (29), the mice were kept in a heterozygous state ($Cyp24a1^{+/-}$). To knockout *Cyp24a1* inTPO-$Braf^{V600E}$ mice, $Cyp24a1^{+/-}$ mice were first crossed with *LSL-*$Braf^{V600E}$ or TPO-Cre mice to generate a $Cyp24a1^{+/-}$; $Braf^{V600E}$ strain or TPO-Cre; $Cyp24a1^{+/-}$ strain. $Cyp24a1^{+/-}$; $Braf^{V600E}$ mice and TPO-Cre; $Cyp24a1^{+/-}$ mice were then bred together to create TPO-$Braf^{V600E}$-$Cyp24a1^{-/-\ or\ null}$ mice. Female athymic BALB/c-nu/nu mice (6–10 weeks of age) were acquired from The Jackson Laboratory. Mice were provided with autoclaved food and water *ad libitum*. The study was approved by the Animal Care and Use Committee of the institution and conducted in compliance with the Public Health Service Guidelines for the Care and Use of Animals in Research.

Genotyping of transgenic mice

The genotyping of Cre-mediated recombination of the LSL-$Braf^{V600E}$ targeted allele has been described previously (27). Briefly, the following primers were used to detect *LSL-*$Braf^{V600E}$ recombination in the mouse tissue: primer A, 5′-AGTCAATCA TCCACAGAGACCT-3′; primer B, 5′-GCTTGGCTGGACGTAAA-CTC-3′; and primer C, 5′-GCCCAGGCTCTTTATGAGAA-3′. Primers A + C detected the wild-type allele (466 bp) and Cre-recombined $Braf^{V600E}$ allele (518 bp). Primers B + C detected the *LSL-*$Braf^{600E}$ allele (140 bp). For genotyping the *Cyp24a1*- knockout mice, the following primers were used: primer 1, 5′-GCAGCATCTCCACAGGTTCACTGTC-3′; primer 2, 5′-AAGAT-CAACCCCTTCGCTCATCTCC-3′; and primer 3, 5′-CGCATCGC-CTTCTATCGCCTTC-3′. Primers 1 + 2 detected the wild-type allele of 250 bp, and primers

1 + 3 detected the mutant allele of 600 bp. The PCR conditions were as follows: 94°C for 5 minutes followed by 35 cycles of amplification (94°C for 30 seconds, 58°C for 30 seconds, 72°Cfor 1 minutes) with a final extension at 72°C for 10 minutes.

Establishment of thyroid tumor cell lines

Thyroid tumors were collected aseptically from donor mice ($BVE^{Cyp24a1\text{-}wt}$ and $BVE^{Cyp24a1\text{-}wll}$) using blunt dissection, then mechanically dissociated by mincing and passing through a 40μm/mesh sterile screen, and suspended in DMEM/F12 growth medium (10% fetal bovine serum, 100 units/mL penicillin, 100 μg/mL streptomycin). The cells were further dissociated by incubation in growth medium containing 100 U/mL type I collagenase (Sigma-Aldrich) and 1.0 U/mL dispase I (Roche Diagnostics) at 37°C in a rocking water bath for 60 minutes. The cell suspension was washed twice with growth media and resuspended in a 10mm culture dish with DMEM/F12 growth medium containing 4 mU/mL bovine TSH (Sigma-Aldrich) to establish $BVE^{Cyp24a1\text{-}wt}$ and $BVE^{Cyp24a1\text{-}null}$ cell lines. The established cell lines were propagated in DMEM/Ham's F12 growth medium. Two cell lines were established each from two separate $BVE^{Cyp24a1\text{-}wt}$ or $BVE^{Cyp24a1\text{-}null}$ primary thyroid tumors in 2015: $BVE^{Cyp24a1\text{-}wt}$-1, $BVE^{Cyp24a1\text{-}wt}$-2, $BVE^{Cyp24a1\text{-}null}$-1, and $BVE^{Cyp24a1\text{-}null}$-2. The thyroid origin of these cell lines was confirmed by genotyping in the lab as described above, which was performed 1 month before using the cell lines.

Quantitative real-time RT-PCR analysis for *Cyp24a1* expression

Total RNA was isolated from the thyroid tumor tissues of $BVE^{Cyp24a1\text{-}wt}$ mice and $BVE^{Cyp24a1\text{-}null}$ mice by the quanidinium thiocyanate-phenol-chloroform method (32). The integrity of the RNA was verified by denaturing gel electrophoresis. Two micrograms (μg) of each total RNA was reverse-transcribed to cDNA using the Promega RT system (Promega). The LightCycler DNA Master SYBR Green 1 Kit was used for quantitative real-time PCR analysis (33). The cDNA mix was diluted 10-fold, and 2 mL of the dilution was used for real-time PCR analysis. The PCR primers for the 126-bp *Cyp24a1* cDNA fragment were: 5′-CATCGCAAC-GAAGCCTACGGG-3′ (sense, located in exon 2) and 5′-CTCATT-GATTTTCTTGTCCAGC-3′ (antisense, located in exon 3). The sense primer spans over 756 bp intron 2 so that the contaminated genomic DNA would not be amplified. The *Cyp24a1* cDNA fragment was verified by DNA sequencing. The mRNA level of the housekeeping gene *Actb* (β-actin) was used as an internal control, and a 180-bp PCR product was amplified using the following two primers: 5′-AAATCGTGCGTGACATCAAA-3′ (sense) and 5′-AAGGAAGGCTGGAAAA GAGC-3′ (antisense). The PCR conditions are 94°C for 30 seconds followed by 30 cycles of amplification (94° C for 10 seconds, 48° C for 5 seconds, and 72°C for 10 seconds). The resulting concentration of *Cyp24a1* PCR products was normalized by comparison with b-actin and was used to determine the relative mRNA level of *Cyp24a1* in the thyroid tumors (ddCt method; ref. 33).

Thyroid stimulating hormone measurements

Blood was collected by cardiac puncture. Serum thyroid stimulating hormone (TSH) was measured using the MILLIPLEX MAP Mouse Pituitary Magnetic Bead Panel following the manufacturer′s instructions (EMD Millipore Corporation).

Histology and immunohistochemistry

Histology and immunohistochemical staining were performed as described previously (34). Briefly, 4-mm-thick formalin-fixed paraffin-embedded tissue sections were prepared and stained with hematoxylin and eosin (H&E) or with a Ki67 antibody (1:100 dilution, ab16667, Abcam). ADAKO LSAB + kit using horseradish peroxidase (HRP) was used for immunostaining (DAKO). The sections were counterstained with Mayer's hematoxylin.

Cloning and expression of *Cyp24a1* in BVE$^{Cyp24a1\text{-}null}$ cells

The *Cyp24a1* cDNA was cloned into pcDNA3.1 as described previously (35). The expression construct was transfected into the BVE$^{Cyp24a1\text{-}null}$ cell line using Lipofectamine (Invitrogen) and selected for 4 weeks with 400 μg/mL zeocin. Stable clones were pooled and used for subsequent experiments.

Western blot analysis

Cell lysates were obtained by extraction in RIPA buffer (20 mmol/L Tris-HCl, pH7.4, 150 mmol/L NaCl, 5 mmol/L EDTA, 1% NP-40) containing Pierce's Halt Protease Inhibitor Cocktail (Thermo Scientific). The protein concentration was determined by Bradford's assay using a Bio-Rad protein assay kit (Bio-Rad). The proteins (40 μg) were separated on a 12% SDS-polyacrylamide gel and then transferred to a PVDF membrane. Western blot analysis was performed using antibodies (1:1000 dilution, Cell Signaling Technology, Inc.) against phospho-Erk 1/2 (#4370), phosphor-Akt (#4060), p-Smad2 (#3101), E-cadherin (#3195), Snail (#3879), vimentin (#5741), and vitamin D receptor (#12550), or antibodies against Zeb1 (1:1000 dilution, sc-25388,Santa Cruz Biotechnology), orCYP24A1 (1:1000 dilution, ab 109632, Abcam).

Wound-healing assay

Cells were seeded in 6-well plates (10^5 cells/well), and a linear scratch was created with a sterile pipette tip when cells reached confluent monolayer. The cells were rinsed three times with medium to remove cellular debris. Cell migration or wound-healing was monitored by microscopy after 16-hour culture.

Cell proliferation assay

Cell proliferation was measured by a nonradioactive MTT assay kit according to the manufacturer's procedure (Promega Corp). Briefly, the cells were plated in triplicate into 96-well plates (10^3 cells/well) in growth medium containing vehicle (0.5% DMSO), different concentrations of calcitriol (Sigma-Aldrich), PLX4720 (Selleck Chemicals), or both for up to 72 hours. For the final 4 hours of incubation, 20 μL of CellTiter 96 AQueous One Solution reagent was added into each well for the measurement of cell viability.

Colony formation assay

Cells were plated into 12-well plates (5×10^2 cells/well) and cultured for 14 days in the presence of different concentrations of calcitriol, PLX4720, or both. The cells were then fixed with methanol for 10 minutes and stained with 0.5% crystal violet dye (in methanol:deionized water, 1:5) for 10 minutes. After three washes with deionized water to

remove excess crystal violet dye, the crystal violet dye was released from the cells by incubation with 1% SDS for 2 hours before optical density $(OD)_{570\ nm}$ measurement.

RNA sequencing for quantification of differentially expressed genes

Total RNA from $BVE^{Cyp24a1\text{-}wt}$-1 and $BVE^{Cyp24a1\text{-}null}$-1 cell lines was isolated, and libraries were constructed using an Illumina TruSeq RNA Library Prep kit according to the manufacturer's procedure. All sequencing was performed on Illumina HiSeq 4000 with at least 20 million clean reads. The significant differentially expressed genes (DEG) were selected based on the following criteria: Log_2-fold change >2, false discovery rate (FDR) <0.001, and *P* value from difference test < 0.01. Selected DEGs were verified by qRT-PCR, and their primer sequences are provided in Supplementary Table S1.

Statistical analysis

Student *t* test (two-tailed) was used to compare two groups, and one-way ANOVA was used to compare multiple groups. A *P* value of 0.05 or less was considered statistically significant.

Results

Reduction of thyroid tumor growth in $BVE^{Cyp24a1\text{-}null}$ mice

We examined *Cyp24a1* expression by qRT-PCR in normal thyroid tissues from 8 *TPO-*$Braf^{WT}$ mice and 2 thyroid tumors from different age groups of $BVE^{Cyp24a1\text{-}wt}$ mice (from 1 to 6 months old). Consistent with our previous findings in human PTC, the *Cyp24a1* expression was increased by more than 3 times in 1-month-old thyroid tumors from both male and female mice with $Braf^{V600E}$ mutation. The *Cyp24a1* expression was gradually increased as they aged up to 7 to 9 times in 6-month-old tumors as compared with normal thyroids (Fig. 1A, $P < 0.001$). To investigate the effect of *Cyp24a1* overexpression on thyroid tumor growth in the presence of the $Braf^{V600E}$ mutation, we knocked out the *Cyp24a1* gene by cross-breeding $BVE^{Cyp24a1\text{-}wt}$ mice with $Cyp24a1^{nuU}$ mice. The *Cyp24a1* knockout was confirmed by genotyping (Fig. 1B). As shown in Fig. 1C, thyroid tumor growth was significantly reduced in $BVE^{Cyp24a1\text{-}null}$ compared with $BVE^{Cyp24a1\text{-}wt}$ mice. Among 12 age- and sex-matched pairs (3 pairs in each group), the thyroid tumor load at different ages was reduced by an average of 4-fold in $BVE^{Cyp24a1\text{-}null}$ mice (35.00 ± 11.73 mg vs. 127.5 ± 43.78 mg in $BVE^{Cyp24a1\text{-}wt}$ mice, $P < 0.05$, Fig. 1C). The papillary architecture of thyroid tumors was lost and replaced by a more compact structure with reduced immunostaining of the cell proliferation marker Ki67 (Fig. 1D). These observations were not found in the heterozygous *Cyp24a1*-knockout mice carrying the $Braf^{V600E}$ mutation (data not shown). The phenotype of $BVE^{Cyp24a1\text{-}null}$ mice was similar to that of $BVE^{Cyp24a1\text{-}wt}$ mice, and their body weight was approximately half of the normal mice. Both $BVE^{Cyp24a1\text{-}null}$ and $BVE^{Cyp24a1\text{-}wt}$mice had severe hypothyroidism with elevated levels of serum TSH greater than 50,000 pg/mL ($n = 5$), which was beyond the detection limit of the assay and more than 100-fold higher than normal TPO-$Braf^{WT}$ mice (n = 5, 394.3 ± 8.7 pg/mL). These data indicate that the loss of *Cyp24a1* had no impact on hypothyroidism caused by the $Braf^{V600E}$ mutation.

Tumorigenicity of BVE$^{Cyp24a1\text{-}null}$-derived tumor cells

Due to impaired vitamin D catabolism, 50% of *Cyp24a1*^{null} mice died before 3 weeks of age (29, 36). A similar mortality rate was found in BVE$^{Cyp24a1\text{-}null}$ mice, and the remaining mice could live up to 6 months. Because we could not maintain sufficient numbers of BVE$^{Cyp24a1\text{-}null}$ mice to evaluate the long-term effect of *Cyp24al*-knockout on tumorigenicity and survival, we instead established thyroid tumor cell lines from BVE$^{Cyp24a1\text{-}null}$ and BVE$^{Cyp24a1\text{-}wt}$ mice and injected them subcutaneously into nude mice ($n = 5$) to observe tumor growth. The BVE$^{Cyp24a1\text{-}null}$ cells expressed neither functional *Cyp24a1* nor responded to calcitriol stimulation to induce *Cyp24a1* expression (Fig. 2A). The residual *Cyp24a1* expression detected by qRT-PCR was likely truncated transcripts (without exon 9 and 10) undergoing nonsense-mediated decay. The CYP24A1 protein was not detected in the BVE$^{Cyp24a1\text{-}null}$ cells and reappeared after transfection of *Cyp24a1* cDNA (Fig. 2B). *Cyp24a1* transcripts from BVE$^{Cyp24a1\text{-}wt}$ cells were significantly increased following 16 hours of calcitriol stimulation (Fig. 2A). However, no change in the CYP24A1 protein level was observed following 100 nmol/L calcitriol stimulation for 48 hours. The elevated protein level was demonstrated after 72 and 96 hours of stimulation (Fig. 2B and C). The delay in protein synthesis after calcitriol stimulation may be due to the feedback inhibition by the already elevated CYP24A1 protein level and/or abrogated vitamin D signaling in the *Braf*^{V600E}--induced thyroid cancer cells. VDR expression was increased in all the cell lines after calcitriol stimulation. The basal level of VDR expression and its induction by vitamin D were reduced in BVE$^{Cyp24a1\text{-}null}$-1 cells (Fig. 2B). These data provided evidence that vitamin D signaling was intact and there was no amplification of vitamin D signaling as a result of *Cyp24a1* deletion. As shown in Fig. 2D, the tumorigenicity of BVE$^{Cyp24a1\text{-}null}$ cells from both BVE$^{Cyp24a1\text{-}null}$-1 and BVE$^{Cyp24a1\text{-}null}$-2 cell lines was significantly decreased. The tumor weight at4 weeks after injection of2×10^6 cells was 0.10 ± 0.01 g from BVE$^{Cyp24a1\text{-}null}$-1 cells and 0.09 ± 0.02 g from BVE$^{Cyp24a1\text{-}null}$-2 cells vs. 1.90 ± 0.17 g from BVE$^{Cyp24a1\text{-}wt}$-1 cells and 1.97 ± 0.39 g from BVE$^{Cyp24a1\text{-}wt}$-2 cells ($P < 0.001$), a 19-fold reduction in the tumorigenic potential (Fig. 2D and E). The tumorigenic potential was partially recovered after reexpression of wild-type *Cyp24a1* in the BVE$^{Cyp24a1\text{-}null}$-1 cells (0.1 ± 0.01 g in BVE$^{Cyp24a1\text{-}null}$-1 vs. 0.51 ± 0.09 g in BVE$^{Cyp24a1\text{-}null}$-1Cyp24a1, $P < 0.001$; Fig. 2D and E).

Reduction in MAPK, PI3K/Akt, and TGFp signaling pathways in the BVE$^{Cyp24a1\text{-}null}$-derived tumor cells

To investigate the mechanisms that resulted in the loss of tumorigenic potential, we studied the p-Erk, p-Akt, and p-Smad2 levels in the two BVE$^{Cyp24a1\text{-}null}$ cell lines established from two separate tumors by Western blot analysis. Increased phosphorylation of these proteins was reported to be associated with tumor progression in thyroid cancer (37, 38). As shown in Fig. 3A, their phosphorylation levels were decreased in both BVE$^{Cyp24a1\text{-}null}$ cell lines. We also found significant reduction of Snail and ZEB1 expression in the BVE$^{Cyp24a1\text{-}null}$ cell lines (Fig. 3B). Both Snail and ZEB1 are zinc finger transcription factors that promote epithelial-mesenchymal transition (EMT) by downregulating the expression of the adhesion molecule E-cadherin (39, 40). As expected, E-cadherin expression was increased and the expression of the mesenchymal cell marker vimentin was not detected (Fig. 3B), indicating that EMT was absent in the BVE$^{Cyp24a1\text{-}null}$ cells. Furthermore, cell migration was reduced

in the BVE$^{Cyp24a1\text{-}null}$ cells (Fig. 3C). To further confirm the reduced p-Erk, p-Akt, and p-Smad2 levels in the BVE$^{Cyp24a1\text{-}null}$ cells was due to decreased *Cyp24a1* expression, we transfected *Cyp24a1* cDNA into the BVE$^{Cyp24a1\text{-}null}$-1 cell line (BVE$^{Cyp24a1\text{-}null}$-1Cyp24a1) to overexpress exogenous CYP24A1. As shown in Fig. 4D, the p-Erk, p-Akt, and p-Smad2 levels were increased, and E-cadherin expression was decreased in the BVE$^{Cyp24a1\text{-}null}$-1Cyp24a1 cells. The reexpression of *Cyp24a1* did not rescue the expression of the EMT marker vimentin. It may take a longer time and/or need a higher level of CYP24A1 to induce its expression. These data demonstrated that CYP24A1 overexpression in Braf mutant cells could upregulate multiple signaling pathways to drive tumor progression.

Synergistic effects of calcitriol and BRAF^{V600E} inhibitor PLX4720 against PTC cells

Because CYP24A1 catabolizes calcitriol, we expected increased calcitriol-mediated growth arrest in BVE$^{Cyp24a1\text{-}nu11}$ cells. To our surprise, we did not find any significant difference in cell proliferation between BVE$^{Cyp24a1\text{-}wt}$-1 and BVE$^{Cyp24a1\text{-}null}$-1 cells before or after calcitriol treatment (Fig. 4). This was confirmed by a nonradioactive MTS assay (200 nmol/L for up to 72 hours, data not shown). Next, we investigated whether the combination of calcitriol and PLX4720 could enhance the antiproliferative effect of PLX4720. Both BVE$^{Cyp24a1\text{-}wt}$-1 and BVE$^{Cyp24a1\text{-}null}$-1 cells were treated with calcitriol or PLX4720 alone or in combination for a short term (up to 72 hours) and long term (14 days). The short-term effects were determined by a nonradioactive MTS assay for cell proliferation, and the long-term effects were measured by a colony formation assay. The synergistic effects were not found during short-term culture (data not shown). A significant reduction in cell proliferation was, however, found during the long-term culture when BVE$^{Cyp24a1\text{-}null}$-1 cells were cultured in the presence of PLX4720 for 14 days (Fig. 4). BVE$^{Cyp24a1\text{-}null}$-1 cells were more sensitive to PLX4720 than BVE$^{Cyp24a1\text{-}wt}$-1 cells: 32% versus 75% viable cells after 8 μmol/L PLX4720 treatment ($P < 0.0001$). Although calcitriol alone had no significant effect, it synergized the antiproliferative effects of PLX4720, resulting in further reduction in cell viability to 9% in BVE$^{Cyp24a1\text{-}null}$-1 cells after combined treatment of 8 μmol/L PLX4720 and 200 nmol/L calcitriol versus 32% from single treatment of 8 μmol/L PLX4720 ($P < 0.0001$, Fig. 4). The synergistic effects could also be demonstrated in BVE$^{Cyp24a1\text{-}wt}$-1 cells: 18% viable cells after combined treatment of 8 μmol/L PLX4720 and 200 nmol/L calcitriol versus 75% viable cells after 8 μmol/L PLX4720 treatment alone ($P < 0.0001$, Fig. 4). Similar results were also observed in the BVE$^{Cyp24a1\text{-}wt}$-2 and BVE$^{Cyp24a1\text{-}null}$-2 cells (data not shown). To further confirm that CYP24A1 overexpression caused resistance to PLX4720, we tested BVE$^{Cyp24a1\text{-}null}$-1Cyp24a1 cell line, which overexpressed the CYP24A1 protein. As shown in Fig. 4, BVE$^{Cyp24a1\text{-}null}$-1Cyp24a1 cells became resistant to PLX4720 treatment: 50% viable cells versus 32% for BVE$^{Cyp24a1\text{-}null}$-1 cells after 8 μmol/L PLX4720 treatment ($P < 0.0002$). The calcitriol-mediated complementary effect was also reduced in BVE$^{Cyp24a1\text{-}null}$-1Cyp24a1 cells: 27% viable cells versus 9% after combined treatment with 8 μmol/L PLX4720 and 200 nmol/L calcitriol ($P < 0.0002$, Fig. 4). The synergistic effects of the combined treatment were still obvious when lower concentrations (2 μmol/L PLX4720 and 50 nmol/L calcitriol) were used in BVE$^{Cyp24a1\text{-}null}$-1 cells: 18% from a combined treatment versus 53% from a single PLX4720 treatment ($P < 0.0001$). In BVE$^{Cyp24a1\text{-}wt}$-1 cells, however, the synergistic effects of combined treatment were not

significant at the concentration of 2 μmol/L PLX4720 and 50 nmol/L calcitriol: 62% from a combined treatment versus 72% from a single PLX4720 treatment ($P = 0.0742$, Fig. 4). The synergistic effects of combined treatment were demonstrated when higher concentrations (4 μmol/L PLX4720 and 100 nmol/L calcitriol) were used: 43% from a combined treatment versus 72% from a single PLX4720 treatment ($P < 0.0013$, Fig. 4). These data demonstrate the significant benefit of calcitriol in combination of PLX4720 for the treatment of *Braf^{V600E}-positive* PTC.

Impact of *Cyp24a1* deletion on vitamin D and non-vitamin D-responsive genes

To investigate the impact of *Cyp24a1* deletion on global gene expression of vitamin D and non-vitamin D-responsive genes, we performed RNA sequencing (RNA-Seq) analysis of BVE$^{Cyp24a1\text{-}wt}$-1 and BVE$^{Cyp24a1\text{-}null}$-1 cells before and after calcitriol stimulation (100 nmol/L for 16 hours). Differentially expressed genes (DEG) with $\log_2$ ratio of BVE$^{Cyp24a1\text{-}wt}$-1 + D3/BVE$^{Cyp24a1\text{-}wt}$-1 > 2 (4-fold difference in gene expression after vitamin D stimulation) were selected as vitamin D-responsive genes. A total of 80 DEGs met the selection criteria as vitamin D-responsive genes and their transcript levels were compared among BVE$^{Cyp24a1\text{-}wt}$-1, BVE$^{Cyp24a1\text{-}wt}$-1+D3, BVE$^{Cyp24a1\text{-}null}$-1, and BVE$^{Cyp24a1\text{-}null}$-1+ D3. There were few significant changes in gene expression among vitamin D-responsive genes between BVE-$^{Cyp24a1\text{-}wt}$-1 and BVE$^{Cyp24a1\text{-}null}$-1 cells: only 33 DEGs (17 down- and 16 upregulated) in BVE$^{Cyp24a1\text{-}null}$-1 cells (Fig. 5A; Supplementary Table S2). Several downregulated genes are known to be involved in tumor progression and metastasis: *AMH112, Efemp1, Gjb2, Krt17, Mmp13, Mmp17*, and *Notum* (Supplementary Table S2). Among 16 upregulated genes, most of them had either unknown functions or their functions were paradoxically related to tumor progression *(Mmp3, Kcnh1*, and *Krt16)* except for *Pdlim2* and *Pigr*, which might play a role in tumor growth inhibition (Supplementary Table S2). Pathway analysis showed potential interactions among *Gjb2, Mmp13, Mmp17, Efemp1*, and *Pdlim2*, affecting the extracellular matrix proteins, matrix metalloproteinase, and EMT (Fig. 6A). By contrast, 761 DEGs did not meet the selection criteria as vitamin D-responsive genes and were considered as non-vitamin D-responsive genes: 193 upregulated and 568 downregulated in BVE$^{Cyp24a1\text{-}null}$-1 versus BVE$^{Cyp24a1\text{-}wt}$-1 cells. We selected top 100 DEGs with $\log_2$-fold change >6.57 (more than 95-fold difference in gene expression) for further analysis. A distinct pattern of gene expression was demonstrated between BVE$^{Cyp24a1\text{-}wt}$-1 and BVE$^{Cyp24a1\text{-}null}$-1 cells (Fig. 5B). Only 3 vitamin D-responsive genes were present: *Efemp1, Hist2h2aa2*, and *Ppp1r2-ps3*. The genes reported to be involved in tumor growth/progression or invasion/metastasis are listed in Table 1. Their relevant functions are provided in Supplementary Tables S2 and S3. We verified 13 DEGs from Table 1 by qRT-PCR and the results were consistent with the RNA-Seq data (Fig. 5C and D). Many of these genes are involved in the regulation of β-catenin/Wnt *(Tff1*↑, *Olfm4*↑, *Fscn1*↓, *Cdh6*↓, *Dkkl1*↓, and *Notum*↓, resulting in downregulation of β-catenin), TGF-beta (Nes↓, *Dlx2*↓*)*, and Notch *(Pdzrn4*↓, *Lnx1*↓, and *Msx1*↑*)* signaling pathways, and may contribute to tumor regression. The significant downregulation of a group of EMT-promoting genes *(Efemp1, Fscn1, Cdh6, Prrx1, Fut4, Hoxd9, Ctsz, Acp5*, and *Nes)* may explain the loss of EMT in the BVE$^{Cyp24a1\text{-}null}$ cells (Fig. 6). Interestingly, many of them are homeobox transcription factors: *Msx1, Cdx2, Hoxd9, Prrx1, Hoxc5, En1*, and *Dlx2*.

Discussion

In the present study, we have demonstrated *in vivo* that CYP24A1 overexpression cooperates with oncogenic $Braf^{V600E}$ to promote thyroid cancer progression. The oncogenic potential of $Braf^{V600E}$ is significantly reduced after *Cyp24a1* knockout. Furthermore, a synergy against thyroid cancer cells is observed between calcitriol and the $BRAF^{V600E}$ inhibitor PLX4720, which may have immediate clinical translation for thyroid cancer patients, especially those who are resistant to targeted therapy by vemurafenib (PLX4032), which is the pharmacologic form of PLX4720 and has the same mode of action as PLX4720.

CYP24A1 overexpression has been reported in many cancers and can lead to the abrogation of growth control mediated by vitamin D. Multiple mechanisms are involved in its overexpression: gene amplification in breast and colon cancers (24, 41), miR-125b downregulation in breast cancer (42), and protein kinase CK2 activation in prostate cancer (43). Its overexpression is associated with poor prognosis in patients with lung (21), esophageal (19), colon (22), and thyroid (16, 23) cancers. These studies have clearly shown that CYP24A1 overexpression can be used as a biomarker for prognosis prediction, but its role in cancer development and progression has not been fully evaluated *in vivo*. The current study provides direct evidence that its overexpression promotes thyroid cancer growth and progression by upregulation of multiple signaling pathways, such as MAPK, PI3K/Akt, TGF-b, and EMT. *Cyp24a1* encodes vitamin D 24-hydroxylase, which catabolizes calcitriol into inactive 1a, 24,25$(OH)_3D_3$. Calcitriol exerts its antiproliferative effects via cross-talk with other signaling pathways, including MAPK, PI3K/Akt, and TGFb (7, 44). The upregulation of multiple signaling pathways may be due to increased degradation of calcitriol by *Cyp24a1* overexpression, but a more plausible explanation would be that *Cyp24a1* may have some intrinsic oncogenic functions apart from catabolizing calcitriol. This hypothesis is supported by the following observations: (i) Calcitriol treatment alone had no significant effect on cell proliferation in *Cyp24a1*-knockout cell line $BVE^{Cyp24a1\text{-}null}$; (ii) The tumor growth of $BVE^{Cyp24a1\text{-}null}$ cells was dramatically reduced in nude mice without an increase in the serum calcitriol level; (iii) The tumor growth in nude mice was partially recovered by transfection of *Cyp24a1* cDNA into $BVE^{Cyp24a1\text{-}null}$ cells; (iv) No significant changes in the expression of vitamin D-responsive genes after *Cyp24a1* knockout whereas many nonvitamin D-responsive genes were affected, including transcription factors, oncogenes, tumor suppressor genes, and genes involved in the immune surveillance and metabolism. These data indicate that calcitriol alone or elevated vitamin D signaling may not have significant impact on thyroid tumor growth of $BVE^{Cyp24a1\text{-}null}$ cells. It is the *Cyp24a1* deletion that likely contributes to the tumor regression. Although the hypothesis remains to be confirmed by further studies, the current study demonstrates that *Cyp24a1* overexpression results in upregulation of multiple signaling pathways for thyroid cancer progression: $Braf^{V600E}$ → *Cyp24a1* overexpression → MAPK, PI3K/Akt, TGF-β, and EMT activation → thyroid cancer progression.

Thyroid tumor growth was reduced by 4-fold in $BVE^{Cyp24a1\text{-}null}$ mice, whereas a 19-fold reduction was found in nude mice following transplantation of $BVE^{Cyp24a1\text{-}null}$ cells. This was probably due to elevated serum TSH in the $BVE^{Cyp24a1\text{-}null}$ mice, which could neutralize the beneficial effects of *Cyp24a1* knockout (27). One should bear in mind that

these tumors were subcutaneous and they were not in a similar microenvironment compared with the original tumors. Although tumor growth in nude mice could be affected by locally produced calcitriol, it is unlikely a major contributor for tumor regression given that we did not observe significant reduction of cell proliferation in Cyp24-null cells following calcitriol stimulation. The current study confirmed that *Cyp24a1*-knockout could not reverse the hypothyroidism induced by the $Braf^{V600E}$ mutation. It is known that TSH stimulates thyroid cancer growth and progression, and higher serum TSH is associated with both thyroid cancer incidence and recurrence (45, 46). We have shown previously that chronic TSH stimulation leads to significant hyperplasia and goiter formation, and promotes $Kras^{G12D}$-mediated oncogenic transformation of thyroid follicular cells (34). Due to the high mortality caused by impaired vitamin D catabolism, we could not evaluate survival in the $BVE^{Cyp24a1\text{-}null}$ mice. This needs to be performed in a mouse model with conditional *Cyp24a1* knockout in the thyroid.

The antiproliferative effects of calcitriol were not demonstrated in the $BVE^{Cyp24a1\text{-}null}$ cells. This is likely due to the presence of the $Braf^{V600E}$ mutation, which antagonizes the antiproliferative effects of calcitriol. These effects were clearly shown when combined with the $BRAF^{V600E}$ inhibitor PLX4720. The synergistic effects of calcitriol and PLX4720 have been reported in human thyroid cancer cell lines (23). Given that vemurafenib has recently been approved for the treatment of advanced PTC harboring $BRAF^{V600E}$ mutation, combined treatment may offer better therapeutic outcomes for advanced PTC. A clinical trial may be warranted to test the efficacy of the combined therapy.

Finally, we have uncovered many DEGs that are associated with tumor growth or metastasis by RNA-Seq analysis, whose expression is significantly impacted by *Cyp24a1* knockout. Most of them are non-vitamin D-responsive genes. Vitamin D-responsive genes or their signaling pathways are clearly involved in the antitumor synergy with PLX4720, even though they may not play a major role in the $BVE^{Cyp24a1\text{-}null}$ tumor regression. Because the expression of many non-vitamin D-responsive genes regulating different cellular processes are impacted by *Cyp24a1* knockout, the alteration of these gene is likely to cause downregulation of multiple signaling pathways and the loss of EMT, resulting in tumor regression. Such diverse impacts exerted by *Cyp24a1*- knockout indicate that *Cyp24a1* is a good candidate for targeted cancer therapy.

Supplementary Material

Refer to Web version on PubMed Central for supplementary material.

Acknowledgments

We would like to thank Ms. Roua A Al-Rijjal and Mr. Wilfredo Antiquera for excellent technical support; Mr. Cong Li and Kai Huang from BGI for bioinformatics service.

Grant Support

This study is supported by KACST grant 13-MED1765–20.

The costs of publication of this article were defrayed in part bythe payment of page charges. This article must therefore be hereby marked *advertisement* in accordance with 18 U.S.C. Section 1734 solely to indicate this fact.

References

1. Hundahl SA, Fleming ID, Fremgen AM, Menck HR. A National Cancer Data Base report on53,856 cases of thyroid carcinoma treated inthe U.S., 19851995. Cancer 1998;83:2638–48. [PubMed: 9874472]
2. Kimura ET, Nikiforova MN, Zhu Z, Knauf JA, Nikiforov YE, Fagin JA. High prevalence of BRAF mutations in thyroid cancer: genetic evidence for constitutive activation of the RET/PTC-RAS-BRAF signaling pathway in papillary thyroid carcinoma. Cancer Res 2003;63: 1454–7. [PubMed: 12670889]
3. Cohen Y, Xing M, Mambo E, Guo Z, Wu G, Trink B, et al. BRAF mutation in papillary thyroid carcinoma. J Natl Cancer Inst 2003;95:625–7. [PubMed: 12697856]
4. Xing M BRAF mutation in thyroid cancer. Endocr Relat Cancer 2005;12: 245–62. [PubMed: 15947100]
5. Trump DL, Muindi J, Fakih M, Yu WD, Johnson CS. Vitamin D compounds: clinical development as cancer therapy and prevention agents. Anticancer Res 2006;26:2551–6. [PubMed: 16886663]
6. Holick MF. Vitamin D deficiency. N Engl J Med 2007;357:266–81. [PubMed: 17634462]
7. Deeb KK, Trump DL, Johnson CS.Vitamin D signalling pathways in cancer: potential for anticancer therapeutics. Nat Rev Cancer 2007;7:684–700. [PubMed: 17721433]
8. Bennett RG, Wakeley SE, Hamel FG, High RR, Korch C, GoldnerWS. Gene expression of vitamin D metabolic enzymes at baseline and in response to vitamin D treatment in thyroid cancer cell lines. Oncology 2012;83: 264–72. [PubMed: 22992568]
9. Liu W, Asa SL, Fantus IG, Walfish PG, Ezzat S. Vitamin D arrests thyroid carcinoma cell growth and induces p27 dephosphorylation and accumulation through PTEN/akt-dependent and -independent pathways. Am J Pathol 2002;160:511–9 [PubMed: 11839571]
10. Zinser GM, Suckow M, Welsh J. Vitamin D receptor (VDR) ablation alters carcinogen-induced tumorigenesis in mammary gland, epidermis and lymphoid tissues. J Steroid Biochem Mol Biol 2005;97:153–64. [PubMed: 16111884]
11. Ooi LL, Zhou H, Kalak R, Zheng Y, Conigrave AD, Seibel MJ, et al. Vitamin D deficiency promotes human breast cancer growth in a murine model of bone metastasis. Cancer Res 2010;70:1835–44. [PubMed: 20160035]
12. Beer TM, Ryan CW, Venner PM, Petrylak DP, Chatta GS, Ruether JD, et al. Double-blinded randomized study of high-dose calcitriol plus docetaxel compared with placebo plus docetaxel in androgen-independent prostate cancer: a report from the ASCENT Investigators. J Clin Oncol 2007;25: 669–74. [PubMed: 17308271]
13. Scaranti M, Junior Gde C, Hoff AO. Vitamin D and cancer: does it really matter? Curr Opin Oncol 2016;28:205–9. [PubMed: 26974846]
14. Willyard C Drug developers explore vitamin D benefits without the vitamin. Nat Med 2011;17:9. [PubMed: 21217659]
15. Balla B, Kosa JP, Tobias B, Halaszlaki C, Takacs I, Horvath H, et al. Marked increase in CYP24A1 gene expression in human papillary thyroid cancer. Thyroid 2011;21:459–60. [PubMed: 21385079]
16. Balla B, Tobias B, Kosa JP, Podani J, Horvath P, Nagy Z, et al. Vitamin Dneutralizing CYP24A1 expression, oncogenic mutation states and histological findings of human papillary thyroid cancer. J Endocrinol Invest 2015;38:313–21. [PubMed: 25201000]
17. Parise RA, Egorin MJ, Kanterewicz B, Taimi M, Petkovich M, Lew AM, et al. CYP24, the enzyme that catabolizes the antiproliferative agent vitamin D, is increased in lung cancer. Int J Cancer 2006;119:1819–28. [PubMed: 16708384]
18. Horvath HC, Lakatos P, Kosa JP, Bacsi K, Borka K, Bises G, et al. The candidate oncogene CYP24A1: a potential biomarker for colorectal tumor-igenesis. J Histochem Cytochem 2010;58:277–85. [PubMed: 19901270]
19. Mimori K, Tanaka Y, Yoshinaga K, Masuda T, Yamashita K, Okamoto M, et al. Clinical significance of the overexpression of the candidate oncogene CYP24 in esophageal cancer. Ann Oncol 2004;15:236–41. [PubMed: 14760115]

20. Lopes N, Sousa B, Martins D, Gomes M, Vieira D, Veronese LA, et al. Alterations in Vitamin D signalling and metabolic pathways in breast cancer progression: a study ofVDR, CYP27B1 and CYP24A1 expression in benign and malignant breast lesions. BMC Cancer 2010;10:483. [PubMed: 20831823]
21. Chen G, Kim SH, King AN, Zhao L, Simpson RU, Christensen PJ, et al. CYP24A1 is an independent prognostic marker of survival in patients with lung adenocarcinoma. Clin Cancer Res 2011;17:817–26. [PubMed: 21169243]
22. Sun H, Wang C, Hao M, Sun R, Wang Y, Liu T, et al. CYP24A1 is a potential biomarker for the progression and prognosis of human colorectal cancer. Hum Pathol 2016;50:101–8. [PubMed: 26997443]
23. Zou M, BinHumaid FS, Alzahrani AS, Baitei EY, Al-Mohanna FA, Meyer BF, et al. Increased CYP24A1 expression is associated with BRAF(V600E) mutation and advanced stages in papillary thyroid carcinoma. Clin Endocrinol (Oxf) 2014;81:109–16. [PubMed: 24382015]
24. Albertson DG, Ylstra B, Segraves R, Collins C, Dairkee SH, Kowbel D, et al. Quantitative mapping of amplicon structure by array CGH identifies CYP24 as a candidate oncogene. Nat Genet 2000;25:144–6. [PubMed: 10835626]
25. Stepien T, Krupinski R, Sopinski J, Kuzdak K, Komorowski J, Lawnicka H, et al. Decreased 1–25 dihydroxyvitamin D3 concentration in peripheral blood serum of patients with thyroid cancer. Arch Med Res 2010;41:190–4. [PubMed: 20682176]
26. Laney N, Meza J, Lyden E, Erickson J, Treude K, GoldnerW. The Prevalence of Vitamin D deficiency is similar between thyroid nodule and thyroid cancer patients. Int J Endocrinol 2010;2010:805716. [PubMed: 20016683]
27. Zou M, Baitei EY, Al-Rijjal RA, Parhar RS, Al-Mohanna FA, Kimura S, et al. TSH overcomes Braf(V600E)-induced senescence to promote tumor progression via downregulation of p53 expression in papillary thyroid cancer. Oncogene 2016;35:1909–18. [PubMed: 26477313]
28. Parhar RS, Zou M, Al-Mohanna FA, Baitei EY, Assiri AM, Meyer BF, et al. IL-12 immunotherapy of Braf(V600E)-induced papillary thyroid cancer in a mouse model. Lab Invest 2016;96:89–97. [PubMed: 26501867]
29. St-Arnaud R, Arabian A, Travers R, Barletta F, Raval-Pandya M, Chapin K, et al. Deficient mineralization ofintramembranous bone in vitamin D-24-hydroxylase-ablated mice is due to elevated 1,25-dihydroxyvitamin D and not to the absence of 24,25-dihydroxyvitamin D. Endocrinology 2000;141:2658–66. [PubMed: 10875271]
30. Mercer K, Giblett S, Green S, Lloyd D, DaRocha Dias S, Plumb M, et al. Expression of endogenous oncogenic V600EB-raf induces proliferation and developmental defects in mice and transformation of primary fibroblasts. CancerRes 2005;65:11493–500.
31. Kusakabe T, Kawaguchi A, Kawaguchi R, Feigenbaum L, Kimura S. Thyr-ocyte-specific expression of Cre recombinase in transgenic mice. Genesis 2004;39:212–6. [PubMed: 15282748]
32. Zou M, Baitei EY, Alzahrani AS, Al-Mohanna F, Farid NR, Meyer B, et al. Oncogenic activation of MAP kinase by BRAF pseudogene in thyroid tumors. Neoplasia 2009;11:57–65. [PubMed: 19107232]
33. Zou M, Famulski KS, Parhar RS, Baitei E, Al-Mohanna FA, Farid NR, et al. Microarray analysis ofmetastasis-associated gene expression profiling in a murine model ofthyroid carcinoma pulmonary metastasis: identification of S100A4 (Mts1) gene overexpression as a poor prognostic marker for thyroid carcinoma. J Clin Endocrinol Metab 2004;89:6146–54. [PubMed: 15579771]
34. Zou M, Baitei EY, Al-Rijjal RA, Parhar RS, Al-Mohanna FA, Kimura S, et al. KRAS(G12D)-mediated oncogenic transformation of thyroid follicular cells requires long-term TSH stimulation and is regulated by SPRY1. Lab Invest 2015;95:1269–77. [PubMed: 26146959]
35. Baitei EY, Zou M, Al-Mohanna F, Collison K, Alzahrani AS, Farid NR, et al. Aberrant BRAF splicing as an alternative mechanism for oncogenic B-Raf activation in thyroid carcinoma. J Pathol 2009;217:707–15. [PubMed: 19156774]
36. St-Arnaud R Targeted inactivation ofvitamin D hydroxylases in mice. Bone 1999;25:127–9. [PubMed: 10423037]
37. Knauf JA, Sartor MA, Medvedovic M, Lundsmith E, Ryder M, Salzano M, et al. Progression of BRAF-induced thyroid cancer is associated with epithelial-mesenchymal transition requiring

concomitant MAP kinase and TGFbeta signaling. Oncogene 2011;30:3153–62. [PubMed: 21383698]

38. Liu Z, Hou P, Ji M, Guan H, Studeman K, Jensen K, et al. Highly prevalent genetic alterations in receptor tyrosine kinases and phosphatidylinositol 3-kinase/akt and mitogen-activated protein kinase pathways in anaplastic and follicular thyroid cancers. J Clin Endocrinol Metab 2008;93:3106–16. [PubMed: 18492751]
39. Hardy RG, Vicente-Duenas C, Gonzalez-Herrero I, Anderson C, Flores T, Hughes S, et al. Snail family transcription factors are implicated in thyroid carcinogenesis. Am J Pathol 2007;171:1037–46. [PubMed: 17724139]
40. Chiu LY, Hsin IL, Yang TY, Sung WW, Chi JY, Chang JT, et al. The ERK-ZEB1 pathway mediates epithelial-mesenchymal transition in pemetrexed resistant lung cancer cells with suppression by vinca alkaloids. Oncogene 2017;36:242–53. [PubMed: 27270426]
41. Hobaus J, Hummel DM, Thiem U, Fetahu IS, Aggarwal A, Mullauer L, et al. Increased copy-number and not DNA hypomethylation causes overexpression of the candidate proto-oncogene CYP24A1 in colorectal cancer. Int J Cancer 2013;133:1380–8. [PubMed: 23463632]
42. Komagata S, Nakajima M, Takagi S, Mohri T, Taniya T, Yokoi T. Human CYP24 catalyzing the inactivation of calcitriol is post-transcriptionally regulated by miR-125b. Mol Pharmacol 2009;76:702–9. [PubMed: 19570947]
43. Luo W, Yu WD, Ma Y, Chernov M, Trump DL, Johnson CS. Inhibition of protein kinase CK2 reduces cyp24a1 expression and enhances 1,25-dihy-droxyvitamin d3 antitumor activity in human prostate cancer cells. Cancer Res 2013;73:2289–97. [PubMed: 23358686]
44. Vuolo L, Di Somma C, Faggiano A, Colao A. Vitamin D and cancer. Front Endocrinol (Lausanne) 2012;3:58. [PubMed: 22649423]
45. Kim HK, Yoon JH, Kim SJ, Cho JS, Kweon SS, Kang HC. HigherTSH level is a risk factor for differentiated thyroid cancer. Clin Endocrinol (Oxf) 2013;78:472–7. [PubMed: 22924613]
46. Boelaert K The association between serum TSH concentration and thyroid cancer. Endocr Relat Cancer 2009;16:1065–72. [PubMed: 19620248]

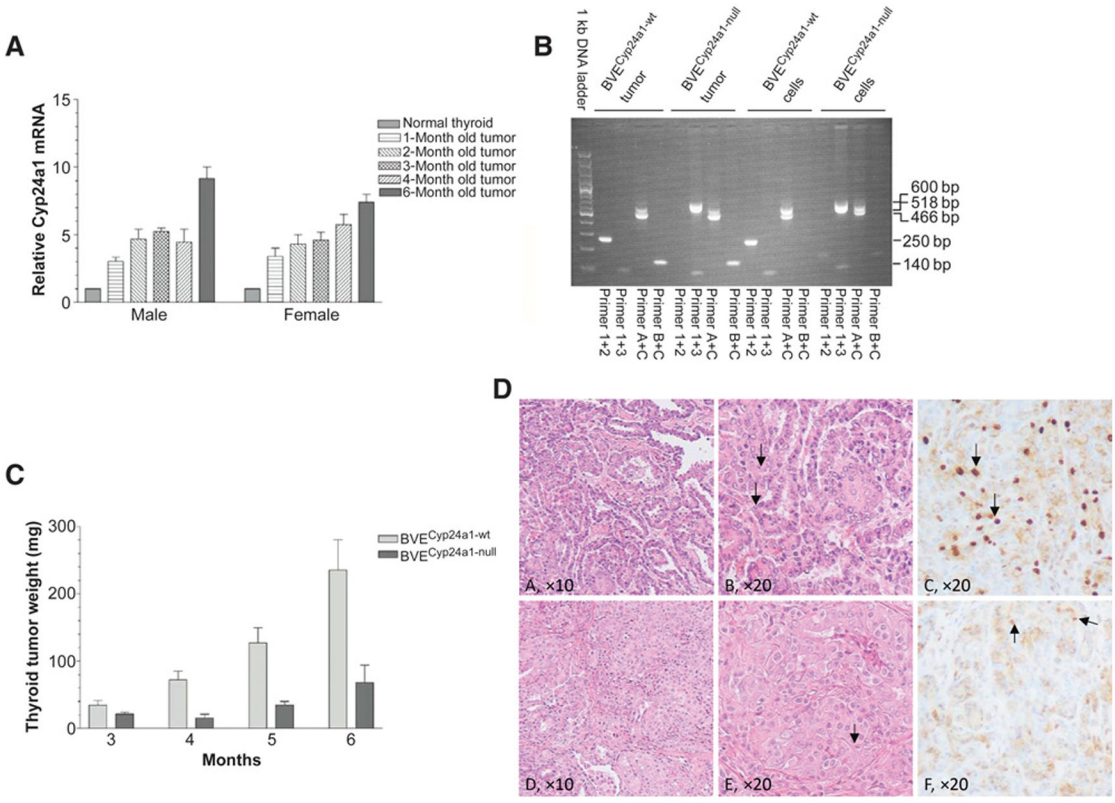

Figure 1.

Cyp24a1 overexpression in BVE$^{Cyp24a1\text{-}wt}$ thyroid tumors and its knockout on thyroid tumor growth. **A**, *Cyp24a1* expression was analyzed by qRT-PCR in normal thyroid tissues from normal control mice (TPO-*Braf*^{WT}; $n = 8$) and thyroid tumors from BVE$^{Cyp24a1\text{-}wt}$ mice ($n = 2$) among different sex and age groups. Data are expressed as the mean ± SEM of relative *Cyp24a1* expression of two tumor samples after normalization to β-actin expression. Results of normal samples were adjusted as 1. *Cyp24a1* expression was increased in mouse PTC with *Braf*^{V600E} mutation. **B**, Genotyping of BVE$^{Cyp24a1\text{-}wt}$ and BVE$^{Cyp24a1\text{-}null}$ tumors and tumor-derived cell lines. The PCR products were run on a 1.5% agarose gel. Wild-type and mutant *Cyp24a1* alleles from BVE$^{Cyp24a1\text{-}wt}$ and BVE$^{Cyp24a1\text{-}null}$ tumors or cell lines are shown by 250-bp (detected by primers 1 + 2) and 600-bp (detected by primers 1 + 3) fragments, respectively. Primers A + C detected the wild-type allele (466 bp) and Cre-recombined *Braf*^{V600E} allele (518 bp). Primers B + C detected the LSL–*Braf*^{V600E} allele (140 bp). The 140-bp fragment was not detected in the cell lines, indicating complete Cre-mediated recombination and thyroid cell origin. **C,** Thyroid tumor growth in BVE$^{Cyp24a1\text{-}null}$ mice. Thyroid tumor growth was compared among 12 age-and sex-matched pairs (three in each group) of BVE$^{Cyp24a1\text{-}null}$ and BVE$^{Cyp24a1\text{-}wt}$ mice for up to 6 months. Thyroid tumor growth was significantly reduced in BVE$^{Cyp24a1\text{-}null}$ mice ($P < 0.05$). **D,** Histology and immunohistochemical staining of thyroid tumors in BVE$^{Cyp24a1\text{-}wt}$ and BVE$^{Cyp24a1\text{-}null}$ mice. The papillary architecture of PTC (**A**; ×10; H&E); characteristic nuclear features of PTC: nuclear grooves, clear or empty nuclei, and nuclear irregularity, indicated by an arrow (**B**;×20; H&E), and immunostaining of a cell proliferation marker Ki67, indicated by an arrow (**C**;×20) in BVE$^{Cyp24a1\text{-}wt}$ mice. The papillary architecture of PTC was lost and

replaced by a more compact structure (**D**; ×10; H&E) with preserved nuclear features of PTC, indicated by an arrow (**E**; ×20; H&E) and reduced immunostaining of Ki67 (**F**; ×10) in $BVE^{Cyp24a1\text{-}null}$ mice.

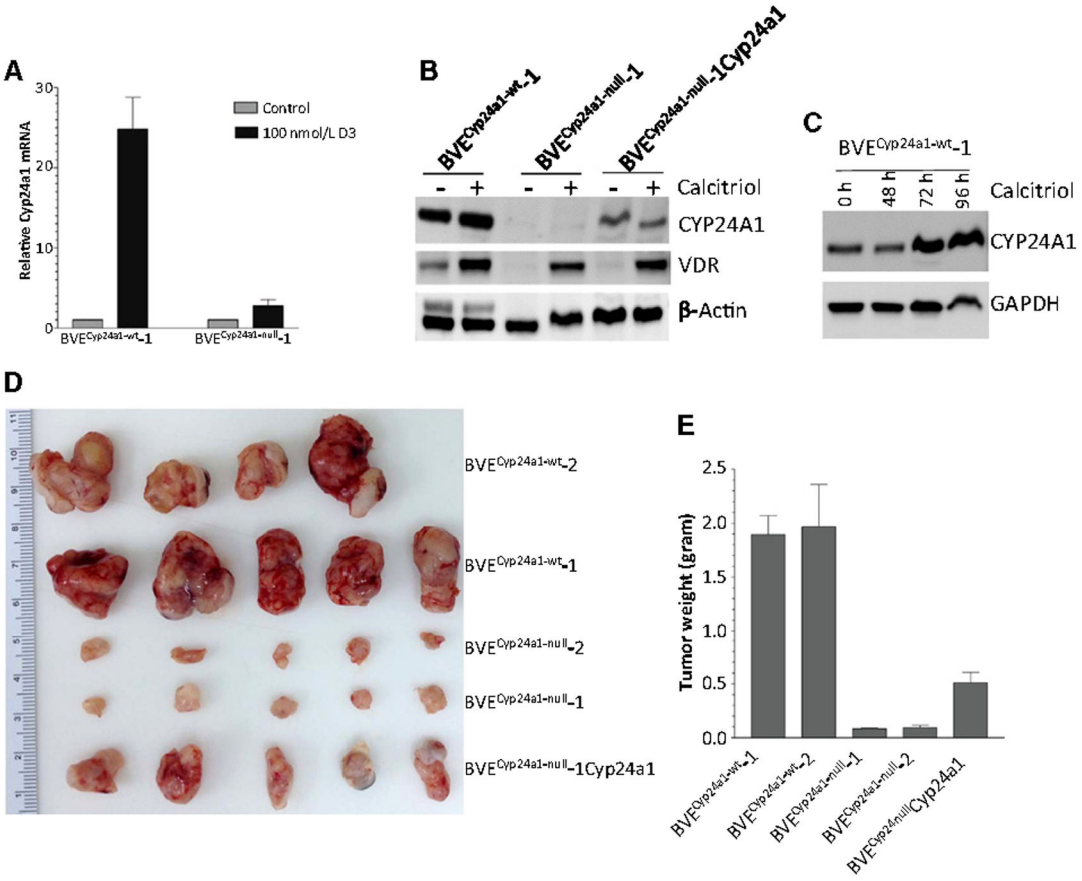

Figure 2.

Tumorigenicity of BVE$^{Cyp24a1\text{-}null}$-derived tumor cells. **A,** Loss of *Cyp24a1* expression in the BVE$^{Cyp24a1\text{-}null}$-derived tumor cells. *Cyp24a1* expression was analyzed by qRT-PCR in cells cultured in the presence or absence of 100 nmol/L calcitriol for 16 hours. The data are expressed as relative expression of *Cyp24a1* after normalization to β-actin expression in each sample. Results of controls were adjusted as 1. **B,** Western blot analysis of CYP24A1 and vitamin D receptor (VDR) expression in BVE$^{Cyp24a1\text{-}wt}$-1, BVE$^{Cyp24a1\text{-}null}$-1, and BVE$^{Cyp24a1\text{-}null}$-1 cells transfected with wild-type Cyp24a1 (BVE$^{Cyp24a1\text{-}null}$-1Cyp24a1). The cells were cultured in the presence or absence of 100 nmol/L calcitriol for 72 hours. **C,** Time course of CYP24A1 protein expression after calcitriol stimulation. BVE$^{Cyp24a1\text{-}null}$-1 cells were cultured in the presence of 100 nmol/L calcitriol for 48, 72, and 96 hours, respectively. The CYP24A1 protein expression was detected by Western blot analysis. **D,** Tumor growth in nude mice following subcutaneous injection of 2×10^6 tumor cells from each of BVE$^{Cyp24a1\text{-}wt}$-1, BVE$^{Cyp24a1\text{-}wt}$-2, BVE$^{Cyp24a1\text{-}null}$-1, BVE$^{Cyp24a1\text{-}null}$-2, or BVE$^{Cyp24a1\text{-}null}$-1Cyp24a1. Four weeks after injection, the tumors were removed, and their weights were measured. **E,** Tumor weight in each group at 4 weeks after injection. Tumorigenic potential was significantly reduced after the loss of CYP24A1 expression. The tumor growth potential was partially restored in the BVE$^{Cyp24a1\text{-}null}$-1 cells following transfection of wild-type *Cyp24a1* expression plasmid.

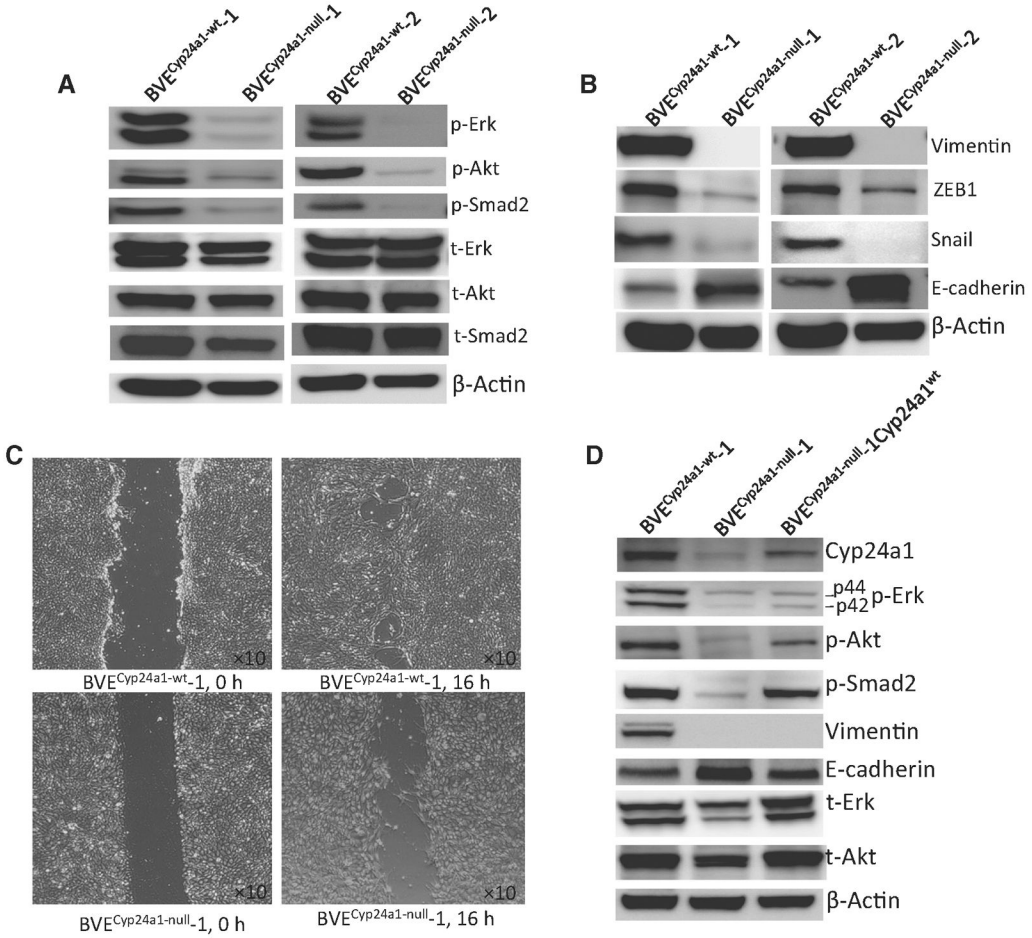

Figure 3.

Cyp24a1 knockout leads to downregulation of the MAPK, PI3K/Akt, TGF-β signaling pathways, and loss of EMT in the BVE$^{Cyp24a1\text{-}null}$-derived tumor cells. **A,** Western blot analysis of the p-Erk, p-AKT, and p-Smad2 protein levels in BVE$^{Cyp24a1\text{-}wt}$-1, BVE$^{Cyp24a1\text{-}wt}$-2, BVE$^{Cyp24a1\text{-}null}$-1, and BVE$^{Cyp24a1\text{-}null}$-2 tumor cell lines. The phosphorylation of these proteins was decreased in both BVE$^{Cyp24a1\text{-}null}$ tumor cell lines. **B,** Western blot analysis of vimentin, ZEB1, Snail, and E-cadherin expression in BVE$^{Cyp24a1\text{-}wt}$-1, BVE$^{Cyp24a1\text{-}wt}$-2, BVE$^{Cyp24a1\text{-}null}$-1, and BVE$^{Cyp24a1\text{-}null}$-2 tumor cell lines. Snail and ZEB1 expression was reduced, whereas E-cadherin expression was increased in both BVE$^{Cyp24a1\text{-}null}$ cell lines. The expression of vimentin was not detected. **C,** Wound-healing assay. Cell migration was measured by the wound-healing assay. Cells were seeded in 6-well plates (10^5 cells/well) and a linear scratch was created when cells reached confluent monolayer. The cells were further cultured for 16 hours to observe wound healing or cell migration. The wound healing or cell migration is reduced in the BVE$^{Cyp24a1\text{-}null}$ cells. **D,** Western blot analysis of the CYP24A1, p-Erk, p-AKT, p-Smad2, vimentin, and E-cadherin protein levels in BVE$^{Cyp24a1\text{-}null}$-1Cyp24a1 tumor cells. Increased phosphorylation of p-Erk, p-AKT, and p-Smad2 and decreased E-cadherin expression are shown in the BVE$^{Cyp24a1\text{-}null}$-1Cyp24a1 tumor cells following reexpression of CYP24A1.

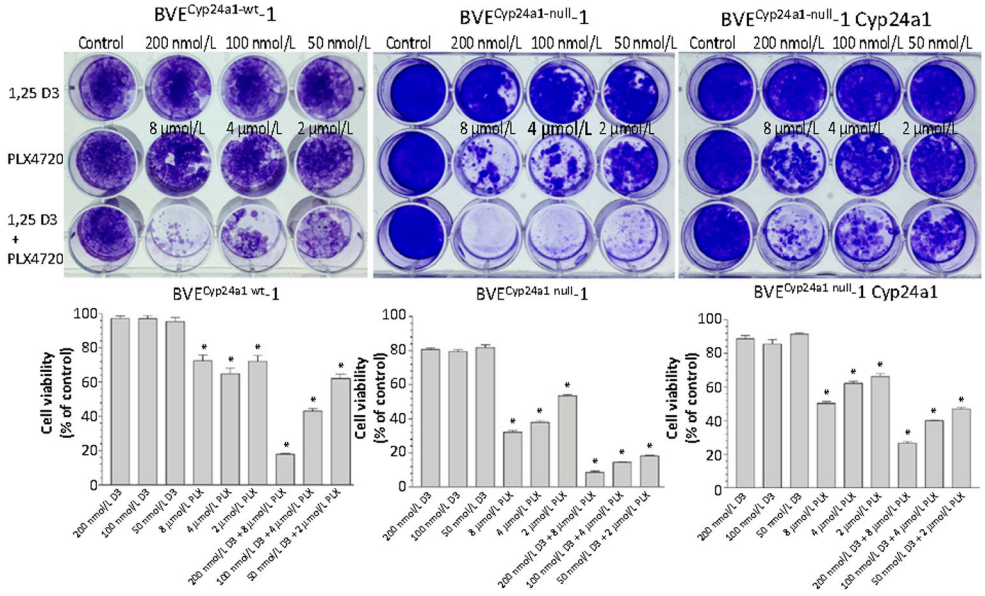

Figure 4.

Effects of calcitriol and the Braf^{V600E} inhibitor PLX4720 on BVE$^{Cyp24a1\text{-}wt}$-1, BVE$^{Cyp24a1\text{-}null}$-1 cells, and BVE$^{Cyp24a1\text{-}null}$-1Cyp24a1 tumor cells. Colony formation assay was used to determine the long-term effects of PLX4720 and calcitriol on cell proliferation. Cells were plated into 12-well plates (5×10^2 cells/well) and cultured in the presence of different concentrations of PLX4720, calcitriol, or both for 14 days. The cells were then stained with 0.5% crystal violet dye (in methanol:deionized water, 1:5) for 10 minutes. After three washes with deionized water, the crystal violet dye was released from the cells by incubation with 1% sodium dodecyl sulfate (SDS) for 2 hours before optical density 570 nm measurement. Cell viability is expressed as a percentage of the vehicle control. *, $P < 0.05$, statistically significant.

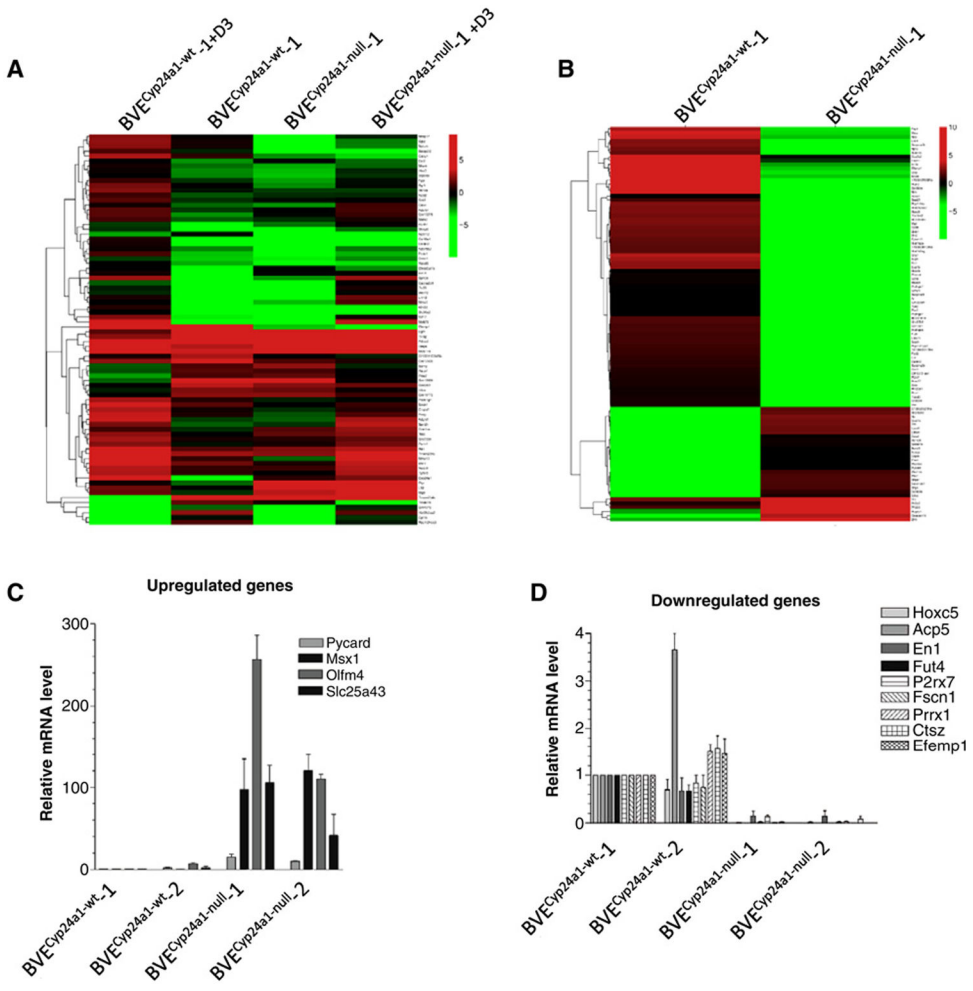

Figure 5.

RNA-Seq analysis of DEGs in the BVE$^{Cyp24a1\text{-}null}$-derived tumor cells. **A,** Heat map of vitamin D–responsive genes in the BVE$^{Cyp24a1\text{-}null}$-1-derived tumor cells. Both BVE$^{Cyp24a1\text{-}wt}$-1 and BVE$^{Cyp24a1\text{-}null}$-1 cell lines were treated with or without 100 nmol/L calcitriol for 16 hours. DEGs with log ratio of BVE$^{Cyp24a1\text{-}wt}$ −1 ± D3/BVE$^{Cyp24a1\text{-}wt}$-1 > 2 were selected as vitamin D–responsive genes. A total of 80 DEGs was included and their expression levels were represented by a color range from green (low) to red (high). No significant changes were observed after *Cyp24a1* deletion. **B,** Heat map of top 100 DEGs in the BVE$^{Cyp24a1\text{-}null}$-1–derived tumor cells. The impact of *Cyp24a1* deletion on the global gene expression was analyzed from 100 highly DEGs (log_2-fold change >6.57). Significant changes in gene expression were demonstrated after *Cyp24a1* deletion. **C,** qRT-PCR analysis of upregulated DEGs in the BVE$^{Cyp24a1\text{-}null}$-1 and BVE$^{Cyp24a1\text{-}null}$-2 cell lines. Data are expressed as the mean ± SEM of the relative mRNA level of target genes after normalization to β-actin expression. Results of BVE$^{Cyp24a1\text{-}wt}$-1 were adjusted as 1. **D,** qRT-PCR analysis of downregulated DEGs in the BVE$^{Cyp24a1\text{-}null}$-1 and BVE$^{Cyp24a1\text{-}null}$-2 cell lines. Data are expressed as the mean ± SEM of the relative mRNA level of target genes after normalization to b-actin expression. Results of BVE$^{Cyp24a1\text{-}wt}$-1 were adjusted as 1.

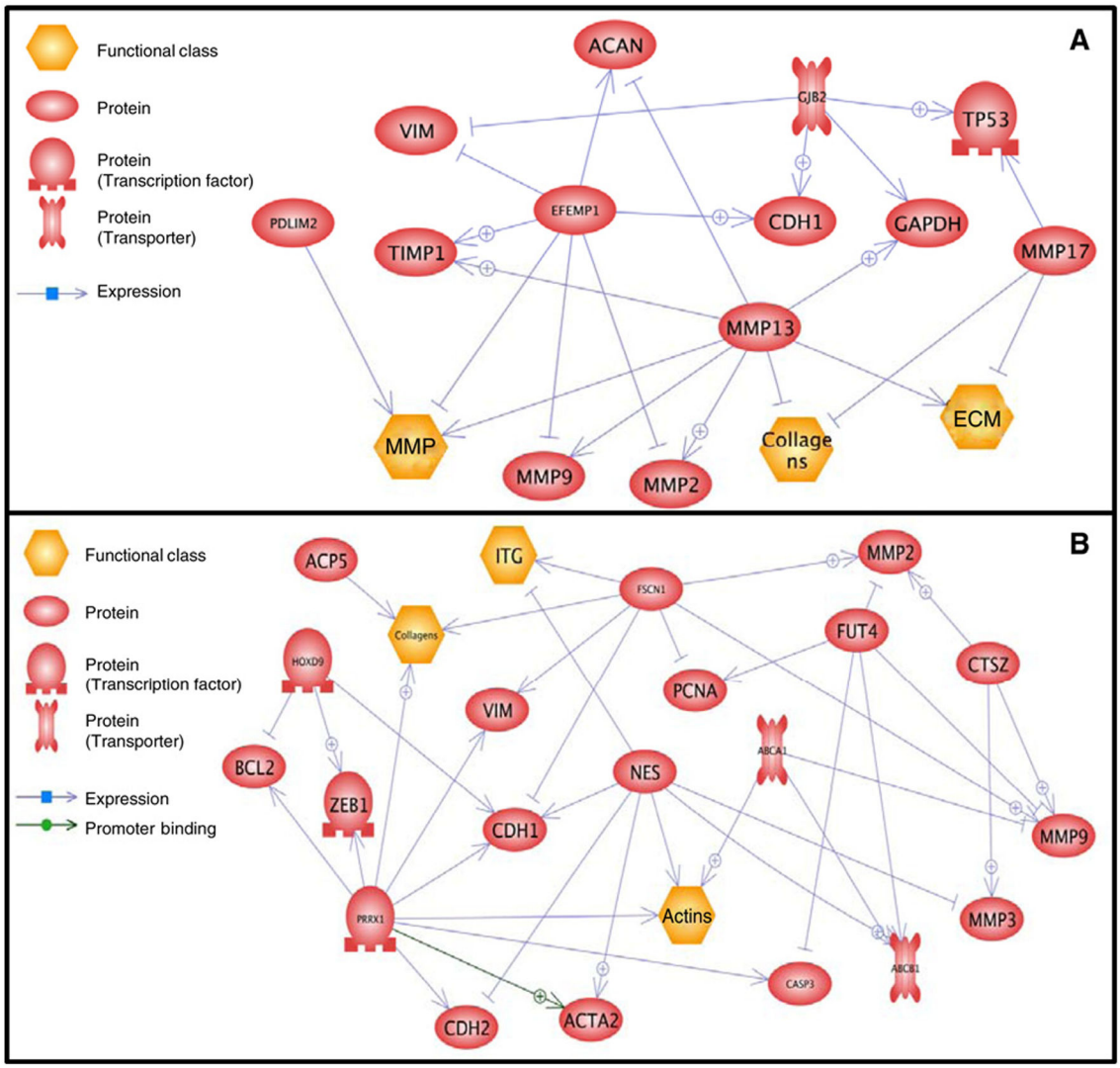

Figure 6.

Potential interactions of genes involved in tumor progression and EMT. **A,** Vitamin D–responsive genes (*Gjb2*, *Mmp13*, *Mmp17*, *Efemp1*, and *Pdlim2*) are shown interacting with CDH1 (E-cadherin), VIM (vimentin), TP53 (P53 tumor suppressor), Acan (aggrecan), Timp1 (tissue inhibitor of metalloproteinases 1), MMP2 (matrix metallopeptidase 2), and MMP9 (matrix metallopeptidase 9). **B,** Non–vitamin D-responsive genes (*Fscn1*, *Acp5*, *Ctsz*, *Prrx1*, *Nes*, *Fut4*, *Abca1*, and *Hoxd9*) are shown interacting with CDH1, CDH2 (N-cadherin), VIM, ACP5 (tartrate-resistant acid phosphatase 5), BCL2 (apoptosis regulator), ZEB1, PCNA (proliferating cell nuclear antigen), ACTA2 (alpha-actin-2), MMP2, MMP9, (matrix metallopeptidase 9), MMP3, and CASP3 (caspase-3). ITG, integrins. The figure was generated by Pathway Studio (https://www.elsevier.com/solutions/pathway-studio-biological-research).

Table 1.

Differentially expressed genes known to be involved in tumor progression and metastasis in the BVE$^{Cyp24a1\text{-}null}$ cells

	Upregulated genes	Downregulated genes
Promote tumor growth and progression	*Clu, Dhh*, ***Kcnh1***	*Ppp1rUa, P2rx7, Hoxc5, Krt20, Foxl2, Lox, Serpina3n, Serpina3i, Csn3*, ***Krt17, Notum***, *En1, Dlx2, Dkkl1, ll17b, Pdzrn4, Lnx1*
Inhibit tumor growth and progression	*Pycard, Slc25a43, Muc5ac, Cdx2*, ***Pigr***	*Crip1 Epb41l3, Pax3, Fez1*
Promote tumor invasion and metastasis	*Cxcl15, Sema7a*, ***Krt16, Mmp3***	*Fscn1, Cdh6, Acp5, Ctsz*, ***Efemp1***, *Nes, Fut4*, ***Aldh1I2, Gjb2, Mmp13, Mmp17***, *Abca1, Hoxd.9*
Inhibit tumor invasion and metastasis	*Tff1, 0lfm4, Msx1 Ffar4*, ***Pdlim2***	*Ndn, Ripk3*
Promote tumor metabolism		*BCO21674, Creb3l4, Pm20d1, Cox6b2, Scnn1b,*
Immune surveillance	*Cd300lb, H2-Q9*	*CD80, Vsir*

NOTE: Vitamin D–responsive genes are highlighted in bold. Detailed information on gene function and references is listed in Supplementary Tables S2 and S3.